BMC Genomics

RESEARCH Open Access

Region-specific transcriptomic responses to *CD52* deficiency in the male reproductive tract

Huifang Kang[1,2*], Yulong Zhu[1], Chunzheng Fu[3], Hao Wang[4], Martien A. M. Groenen[2], Guoying Hua[1*], Lei Huang[1*] and Richard P. M. A. Crooijmans[2]

Abstract

Background Spermatozoa are produced in the testis and acquire motility and fertilizing capacity during post-testicular maturation in the epididymis, a highly region-specific process. How gene loss reshapes region-specific transcriptional programs along the testis–epididymis axis remains poorly defined, particularly in the absence of overt fertility defects. *CD52* is expressed in male reproductive tissues, yet whether *CD52* loss elicits region-specific transcriptomic alterations along the male reproductive tract remains unclear. In this study, we aimed to systematically characterize spatially resolved transcriptomic changes associated with *CD52* deficiency across the testis and epididymal segments.

Results CD52-knockout male mice displayed normal fertility, as assessed by successful mating and offspring production, and showed no obvious histological abnormalities in the testis or epididymis. Multi-region bulk RNA sequencing identified differentially expressed genes in the testis (119), caput epididymis (284), corpus epididymis (577), and cauda epididymis (294). Functional enrichment analyses revealed that pathways related to cytoskeletal organization and motor protein function were predominantly affected in the testis, caput, and cauda. In contrast, pathways associated with cellular homeostasis and ion transport were uniquely enriched in the corpus epididymis. Protein–protein interaction network analysis further identified region-specific hub genes, including *Ttn* in the testis and cauda, *Tcap* in the caput epididymis, as well as *Spp1* in the corpus epididymis. Comparative analyses between adjacent tissues highlighted pronounced transcriptional heterogeneity along the testis–epididymis axis in response to *CD52* deficiency.

Conclusion This study provides a region-resolved transcriptomic characterization of *CD52* deficiency across the testis and epididymal segments. Our findings demonstrate that *CD52* loss is associated with distinct, spatially organized transcriptional responses along the male reproductive tract, offering insight into region-dependent molecular regulation in the absence of overt reproductive phenotypes.

*Correspondence:
Huifang Kang
huifang.kang@wur.nl
Guoying Hua
hgyyxg@163.com
Lei Huang
canoehuang@163.com

Full list of author information is available at the end of the article

Keywords CD52, CRISPR/Cas9, Mouse model, Male reproductive tract, Epididymis segments, Transcriptomics

Introduction

The production of functional male gametes is a complex process that involves spermatogenesis in the testes, followed by post-testicular maturation in the epididymis [1, 2]. Spermatogenesis is a highly coordinated process regulated by precise stage and cell-type-specific gene expression programs within the testis [3, 4]. Spermatozoa leaving the testis are not fully competent and undergo progressive acquisition of motility and fertilizing capacity during transit through the epididymal duct [5–7]. The epididymis is anatomically and functionally segmented into the caput, corpus, and cauda, each characterized by distinct epithelial environments and region-specific gene expression profiles [8–11]. Functional studies indicate that the caput and corpus are primarily involved in early and late maturation processes, respectively, whereas the cauda serves as a storage site for mature spermatozoa [12]. The testis and epididymis constitute a continuous and highly regulated transcriptional axis, providing a valuable in vivo framework for investigating spatial regulation of gene expression underlying sperm development and maturation.

Gene knockout models are widely used to investigate the biological functions of specific genes in male reproduction by comparing testicular and epididymal development, spermatogenesis, and fertility between wild-type (WT) and mutant animals [13, 14]. While deletion of many genes essential for spermatogenesis leads to embryonic lethality or male infertility [15–18], there are also numerous cases in which genetic ablation of testis- or epididymis-enriched genes does not result in overt reproductive phenotypes [19–24]. Importantly, the absence of obvious phenotypic defects does not preclude the presence of underlying molecular or transcriptional alterations. In this context, transcriptome-based analyses across multiple reproductive tissues provide a complementary approach to uncover region-specific molecular responses to gene deletion that may not be evident at the phenotypic level.

CD52 is a glycosylphosphatidylinositol-anchored protein that is widely expressed in immune cells and has also been detected in the male reproductive tract, predominantly in the epididymis [25, 26]. In humans, *CD52* expression has been positively correlated with sperm motility, whereas reduced expression has been observed in individuals with oligozoospermia and asthenozoospermia [27]. *CD52* has also been suggested to be associated with sperm maturation and immunological modulation within the epididymal environment [25], and has been proposed as a sorting marker for human epididymosomes [28]. Notably, previous studies have reported that CD52-deficient mice generated by homologous recombination do not exhibit overt defects in tissue morphology and male fertility under physiological conditions. However, the molecular consequences of *CD52* deficiency in reproductive tissues, particularly in a region-resolved manner along the male reproductive tract, remain poorly characterized.

In this study, we generated a CD52-knockout (CD52-KO) mouse model using CRISPR/Cas9 and performed a multi-region transcriptomic analysis of the male reproductive tract. RNA sequencing was conducted on the testis and three epididymal segments (caput, corpus, and cauda) from WT and CD52-KO male mice. By integrating comparative transcriptomic analyses with functional enrichment and protein–protein interaction (PPI) network analyses, we systematically characterized region-specific transcriptional responses associated with *CD52* deficiency. This study provides a comprehensive transcriptomic resource that highlights spatial heterogeneity along the testis–epididymis axis, thereby offering a framework for understanding region-specific regulatory alterations in the male reproductive tract in the absence of overt reproductive abnormalities.

Materials and methods

Ethics statement

The use and care of animals complied with the guidelines of the Biomedical Research Ethics Committee of the Agricultural Genomics Institute in Shenzhen, Chinese Academy of Agricultural Sciences. Mice were maintained under a 12-hour light/dark cycle at a constant room temperature of 21–23 °C in ventilated cages with ad libitum access to food and water.

Generation of the CD52-KO mice

CD52-KO mice were generated using a CRISPR/Cas9-mediated genome editing approach, as previously described [29]. Briefly, superovulation was induced in 12–15 female C57BL/6J mice (3–4 weeks old) by intraperitoneal injection of pregnant mare serum gonadotropin (PMSG, 5 IU), followed 48 h later by human chorionic gonadotropin (hCG, 5 IU). After hCG administration, females were housed overnight with C57BL/6J males. On the following morning, females with vaginal plugs were identified and used for zygote collection. Zygote–cumulus complexes were treated with hyaluronidase to remove surrounding cumulus cells, washed several times in M2 medium, and cultured in KSOM medium at 37 °C in a humidified incubator with 5% CO_2.

Two single-guide RNAs (sgRNAs) targeting exon 2 of the *CD52* gene were designed using the CHOPCHOP

web tool (https://chopchop.cbu.uib.no/) based on predicted on-target efficiency and minimal off-target potential (Supplementary Table S1). A mixture containing Cas9 mRNA (100 ng/μL) and synthesized sgRNAs (50 ng/μL for each sgRNA) was microinjected into approximately 80 fertilized zygotes. Injected embryos were cultured in KSOM medium for approximately 2.5 days until the blastocyst stage. The resulting blastocysts were subsequently transferred into the oviducts of pseudopregnant ICR recipient females, with 15–20 embryos transferred per recipient. A total of 12 founder mice carrying the intended deletion were obtained.

Genomic DNA was extracted from the tail or foot of the resulting pups. Genotyping was performed using polymerase chain reaction (PCR) and Sanger sequencing to confirm the edit in *CD52*. A 190-bp deletion was introduced in exon 2 of the *CD52* gene, which was validated by PCR and Sanger sequencing and is predicted to cause a frameshift mutation that disrupts the *CD52* coding sequence. The overall workflow of mouse generation and subsequent breeding is illustrated in Supplementary Figure S1.

Breeding strategy

Male CD52-KO founder mice were initially crossed with WT females to generate heterozygous offspring. These heterozygous mice were subsequently backcrossed with WT animals for at least three generations. Heterozygous males and females were then intercrossed to obtain homozygous CD52-KO mice, which were maintained through littermate intercrosses for an additional three generations before experimental use. Genotype distributions among offspring followed expected Mendelian ratios. When multiple eligible male littermates of the same genotype were available, animals were randomly selected for downstream analyses.

Tissue collection

Testis and epididymal segments (caput, corpus, and cauda) were collected simultaneously from age-matched (10-week-old) C57BL/6J WT and CD52-KO male mice ($n = 4$ per group). For downstream analyses, tissues were processed in parallel for either histology or transcriptomic profiling, as described below.

Histology

For histological analysis, freshly dissected tissues were fixed in 4% paraformaldehyde (PFA), embedded in paraffin, and sectioned at 5 μm. Sections were stained with hematoxylin and eosin (H&E) following standard protocols. Specimen sectioning and staining were done by Wuhan Servicebio Technology Co., Ltd. (Wuhan, China). Images were captured using a Leica bright-field microscope system and viewed with NDP.view 2 software.

RNA extraction and transcriptomic analysis

For transcriptomic analysis, tissue samples were snap-frozen in liquid nitrogen and stored at − 80 °C until RNA extraction. All transcriptomic library preparation and sequencing were performed by GENEWIZ, Inc. (Suzhou, China). mRNA libraries were generated through poly(A) mRNA enrichment, RNA fragmentation, reverse transcription using random hexamers or oligo (dT) primers, adaptor ligation, and PCR amplification. High-throughput sequencing was carried out on the DNBSEQ-T7 platform; one corpus epididymis sample failed and was excluded. RNA-seq data generated in this study are available in the NCBI BioProject database under accession number PRJNA1257005 (https://www.ncbi.nlm.nih.gov/bioproject/PRJNA1257005). Sample IDs (e.g., mus-WT-T 1) correspond to the names of the raw data files. Abbreviations: T = testis, H = caput epididymis, EP = corpus epididymis, TA = cauda epididymis.

Raw sequencing reads were assessed for quality using FastQC (version 0.11.2) and then processed with fastp (version 0.22.0) to remove adaptor sequences and low-quality reads [30]. Clean reads were aligned to the mouse reference genome (GRCm39) using STAR (v2.7.10b) [31]. Gene-level read counts were obtained using RSEM (v1.3.1) [32].

Differential gene expression analysis was performed using the DESeq2 package (v1.45.0) [33]. DESeq2 normalization and dispersion estimation were performed using the default DESeq2 pipeline. Differential expression testing was conducted using the Wald test, and p-values were adjusted for multiple testing using the Benjamini–Hochberg false discovery rate (FDR) method. Genes with an adjusted p-value < 0.05 and $|\log2(\text{fold change})| > 1$ were considered differentially expressed. Lowly expressed genes were subject to independent filtering within the DESeq2 framework during multiple testing correction. All samples were processed under uniform experimental conditions. Differential expression analysis was performed using a design formula including genotype as the primary factor (design = ~ genotype, with WT and CD52-KO defined as the two genotype groups).

For Gene Ontology (GO) and Kyoto Encyclopedia of Genes and Genomes (KEGG) enrichment analyses, all expressed genes detected in the corresponding tissue were used as the background gene set. Enrichment analyses were performed using the clusterProfiler package (v4.8.3) [34]. All statistical analyses and data visualization were conducted using R (v4.3.1).

Protein–Protein Interaction (PPI) analysis

PPI networks for DEGs were constructed using the STRING database (v12.0) (https://string-db.org/) [35] with a confidence score threshold > 0.4. Network visualization was performed using Cytoscape (v3.10.2), and

hub genes were identified using the cytoHubba plugin [36].

Results

Generation of *CD52* knockout mice models and reproductive tissue morphology

We generated *CD52* knockout mice by introducing a 190-bp deletion in exon 2 using CRISPR/Cas9, and homozygous KO mice were selected for subsequent experiments (Fig. 1A, Supplementary Fig. S2A–C).

Histological examination of H&E-stained sections revealed no major morphological differences between WT and CD52-KO mice across the testis, caput, corpus, and cauda epididymis (Fig. 1B). The overall epithelial structure and luminal organization were well preserved in both groups.

Sequencing depth and genome mapping rates were examined for all four reproductive tissues (Supplementary Figure S3A–D). Each sample generated approximately 38–55 million reads, with consistently high mapping rates above 85% across both WT and CD52-KO groups, confirming that the RNA-seq libraries were of high quality and suitable for downstream analyses.

In WT mice, *CD52* expression was markedly higher in all epididymal regions compared with the testis, with the strongest expression observed in the cauda region. As expected, *CD52* expression was nearly undetectable across all four tissues in CD52-KO mice (Fig. 1C), confirming the successful knockout of the gene in these tissues.

Transcriptomic alterations in the testis

Transcriptomic profiling of four tissues, including the testis and three epididymis regions (caput, corpus, and cauda), was performed in WT and CD52-KO mice. For the testis analysis, principal component analysis (PCA) revealed a clear separation between the two groups, indicating distinct global transcriptomic profiles (Fig. 2A). Volcano plots visualized the scale and direction of expression changes between groups, including 72 upregulated and 47 downregulated genes in the CD52-KO group compared to WT controls (Fig. 2B). Hierarchical

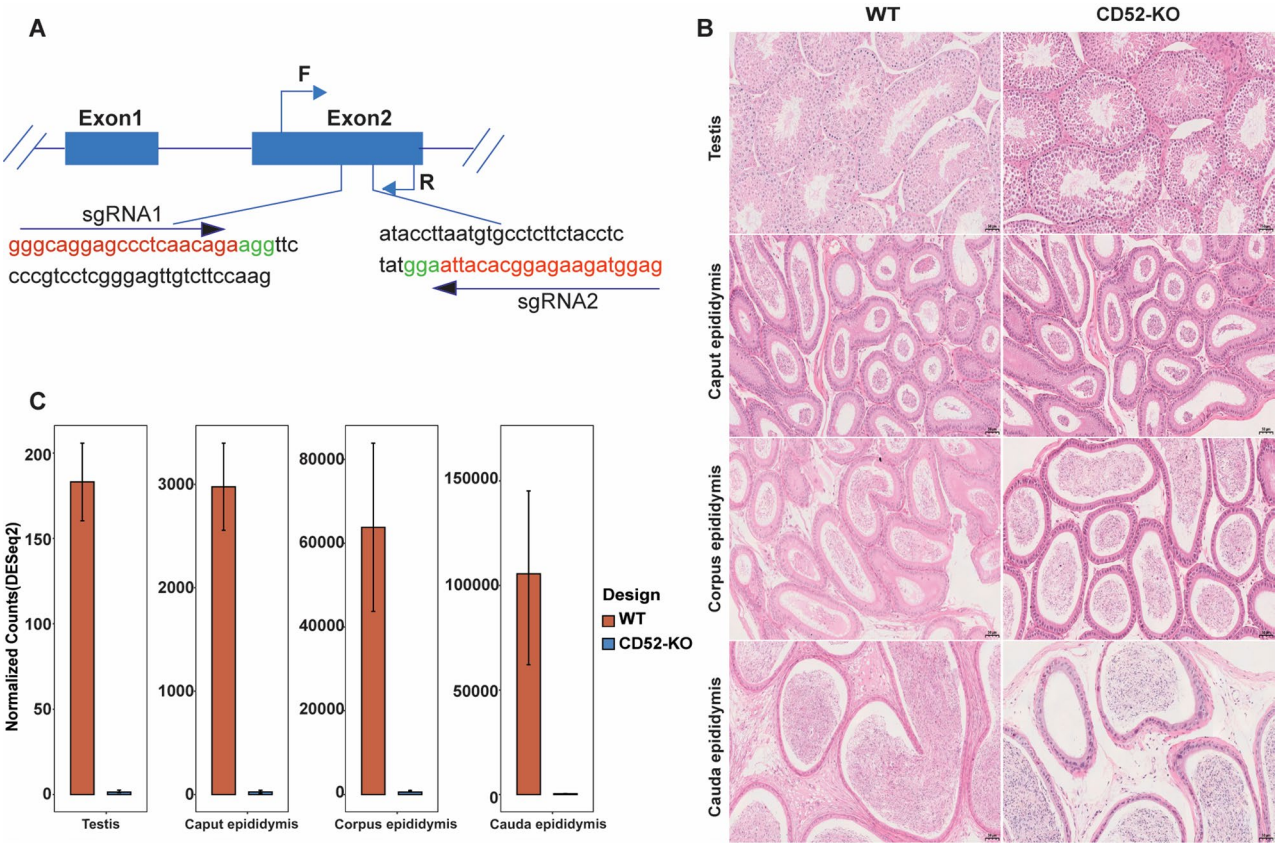

Fig. 1 Generation and tissue morphology evaluation of reproductive tissues in WT and CD52-KO male mice. **A** Schematic diagram of the CRISPR/Cas9-mediated strategy for *CD52* gene knockout. Two sgRNAs, sgRNA1 and sgRNA2, were designed to target exon 2, resulting in a 190 bp deletion (red indicates the sgRNA sequences, green indicates the PAM sequences). Arrows indicate primer positions (F, forward; R, reverse) used for genotyping. **B** Representative H&E-stained tissue sections showing testis and epididymis morphology in WT and CD52-KO mice. Bars, 50 μm. **C** Bar plots showing *CD52* expression levels in the testis and three regions of the epididymis (caput, corpus, and cauda) from WT (red) and CD52-KO (blue) mice based on RNA-seq data. Expression values represent DESeq2-normalized counts

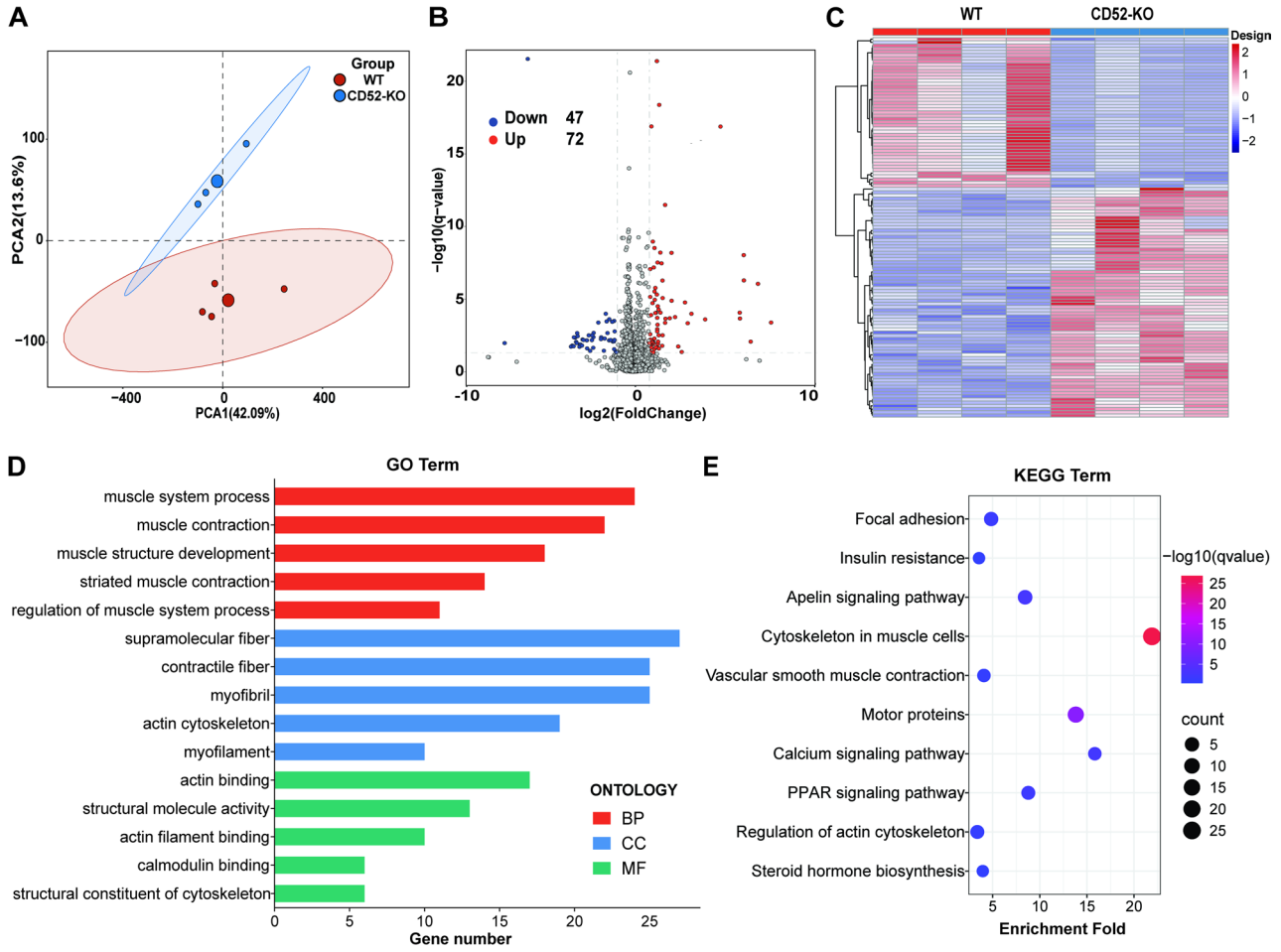

Fig. 2 Transcriptomic analysis of the testis in WT and CD52-KO mice. **A** PCA of gene expression profiles from WT (red) and CD52-KO (blue) testis samples. **B** Volcano plot illustrating the distribution of DEGs between groups (threshold: $|\log_2 FC| > 1$ and adjusted p-value < 0.05). Red and blue dots represent significantly upregulated and downregulated genes in CD52-KO mice, respectively. **C** Heatmap showing hierarchical clustering of DEGs in WT and CD52-KO testes. **D** GO enrichment analysis of DEGs, categorized by biological process (BP), cellular component (CC), and molecular function (MF). **E** KEGG pathway enrichment analysis showing pathways associated with the identified DEGs. Dot size indicates the number of genes; color reflects −log10(q-value)

clustering based on the expression of DEGs also demonstrated a clear distinction between WT and CD52-KO samples, as shown in the heatmap (Fig. 2C).

GO enrichment analysis revealed significant enrichment in terms related to cytoskeletal structure and function, including muscle system process, supramolecular fiber, myofibril, actin binding, and structural constituent of cytoskeleton (Fig. 2D). Additionally, KEGG pathway analysis further highlighted enrichment in cytoskeleton in muscle cells and motor proteins pathway (Fig. 2E). These findings showed that *CD52* deficiency alters gene expression programs related to cytoskeletal organization and contractile function in the testis.

Transcriptomic alterations across epididymal segments

To examine the impact of *CD52* deficiency on the epididymis, we performed transcriptomic profiling of three major regions: the caput, corpus, and cauda epididymis. PCA showed partial separation and genotype-associated clustering trends between WT and CD52-KO samples across all three epididymal segments (Supplementary Figure S4A, D, G), suggesting genotype-associated transcriptomic differences. Volcano plots visualized the scale and direction of expression changes between groups (Supplementary Figure S4B, E, H). Differential expression analyses identified 284 DEGs in the caput (137 upregulated and 147 downregulated), 577 DEGs in the corpus (301 upregulated and 276 downregulated), and 294 DEGs in the cauda (85 upregulated and 209 downregulated), indicating region-specific gene expression changes across all epididymal segments upon *CD52* deletion. Hierarchical clustering based on the expression of DEGs also demonstrated a clear distinction between WT and CD52-KO samples, as shown in the heatmaps (Supplementary Figure S4C, F, I).

In the caput, GO enrichment analysis revealed significant associations with actin binding, supramolecular fiber, and actin cytoskeleton organization

(Supplementary Figure S5A). KEGG analysis further showed enrichment in pathways such as cytoskeleton in muscle cells and motor proteins (Supplementary Figure S5B). In the corpus, GO terms were enriched for cellular homeostasis, supramolecular polymer, and DNA-binding transcription repressor activity (Supplementary Figure S5C). While pathways included cellular senescence, FoxO signaling, and Apelin signaling pathway were enriched in the Corpus epididymis (Supplementary Figure S5D). The cauda showed a functional profile partially overlapping with the caput, with enrichment of GO terms such as actin filament-based process, supramolecular fiber, calcium ion binding, and organelle assembly (Supplementary Figure S5E). Corresponding KEGG analysis included the cytoskeleton in muscle cells and motor proteins (Supplementary Figure S5F).

Taken together, these results demonstrate that *CD52* deficiency alters the transcriptomic landscape across the epididymis in a region-specific manner. The caput and cauda epididymis exhibited similar enrichment patterns related to cytoskeletal structure and dynamics, whereas the corpus epididymis exhibited a distinct transcriptional profile dominated by cellular homeostasis–associated processes.

PPI network analysis

PPI networks were constructed for each tissue, and hub genes were identified based on degree centrality (Fig. 3A–D). In both the testis and cauda epididymis, *Ttn* (Titin) was identified as the hub gene (Fig. 3A, D). The caput epididymis network highlighted *Tcap* (Telethonin, also known as Titin-cap) as the hub gene (Fig. 3B). The corpus epididymis displayed a distinct PPI pattern centered on *Spp1* (Secreted phosphoprotein 1) (Fig. 3C). Consistent with the enrichment results, *Ttn* and *Tcap* were central nodes in networks enriched for cytoskeleton- and motor protein-related pathways, while *Spp1* occupied a central position in networks linked to cellular homeostasis and cell senescence pathways.

Expression analysis further confirmed these patterns (Fig. 3E-H). *Ttn* and *Tcap* were downregulated in the CD52-KO group, while *Spp1* was specifically upregulated in the corpus epididymis. These results highlight the region-specific regulatory programs in response to *CD52* loss, with the testis, caput, and cauda showing convergent enrichment of cytoskeleton-related gene expression patterns, whereas the corpus exhibited a distinct transcriptional profile associated with cellular homeostasis-related processes.

Region-specific transcriptomic divergence along the testis–epididymis axis

Building upon the DEG and enrichment analyses performed for each tissue individually, we next compared DEGs between adjacent regions along the testis–epididymis axis to evaluate spatial transcriptional coordination under *CD52* deficiency. Venn diagram analysis showed that some DEGs were shared between neighboring segments, most were unique to a given region, indicating both common and region-specific transcriptomic responses to *CD52* loss (Fig. 4A–C). Specifically, the testis and caput epididymis shared 56 DEGs (16.2%), the

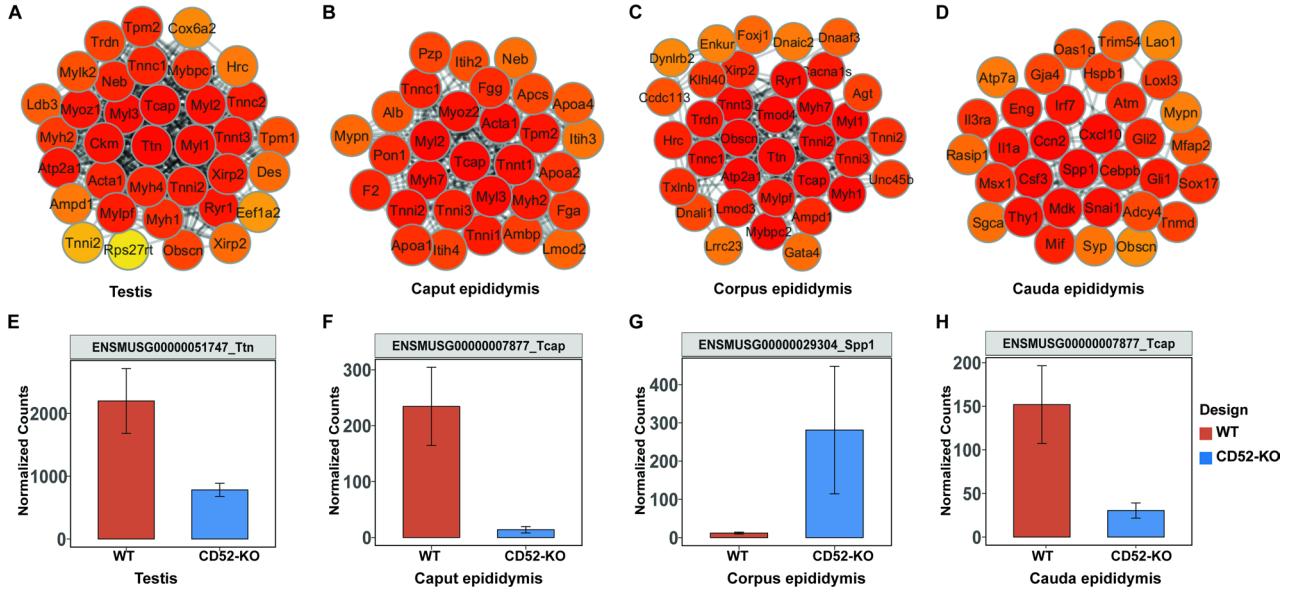

Fig. 3 PPI network and hub gene expression in the testis and epididymis segments. PPI networks constructed from DEGs in the testis (**A**), caput epididymis (**B**), corpus epididymis (**C**), and cauda epididymis (**D**). Node size reflects interaction centrality; hub genes are centrally located. Expression of representative hub genes in WT (red) and CD52-KO (blue) mice: (**E**) *Ttn* in the testis, (**F**) *Tcap* in the caput, (**G**) *Spp1* in the corpus, and (**H**) *Tcap* in the cauda. Error bars represent the standard error of the mean (SEM)

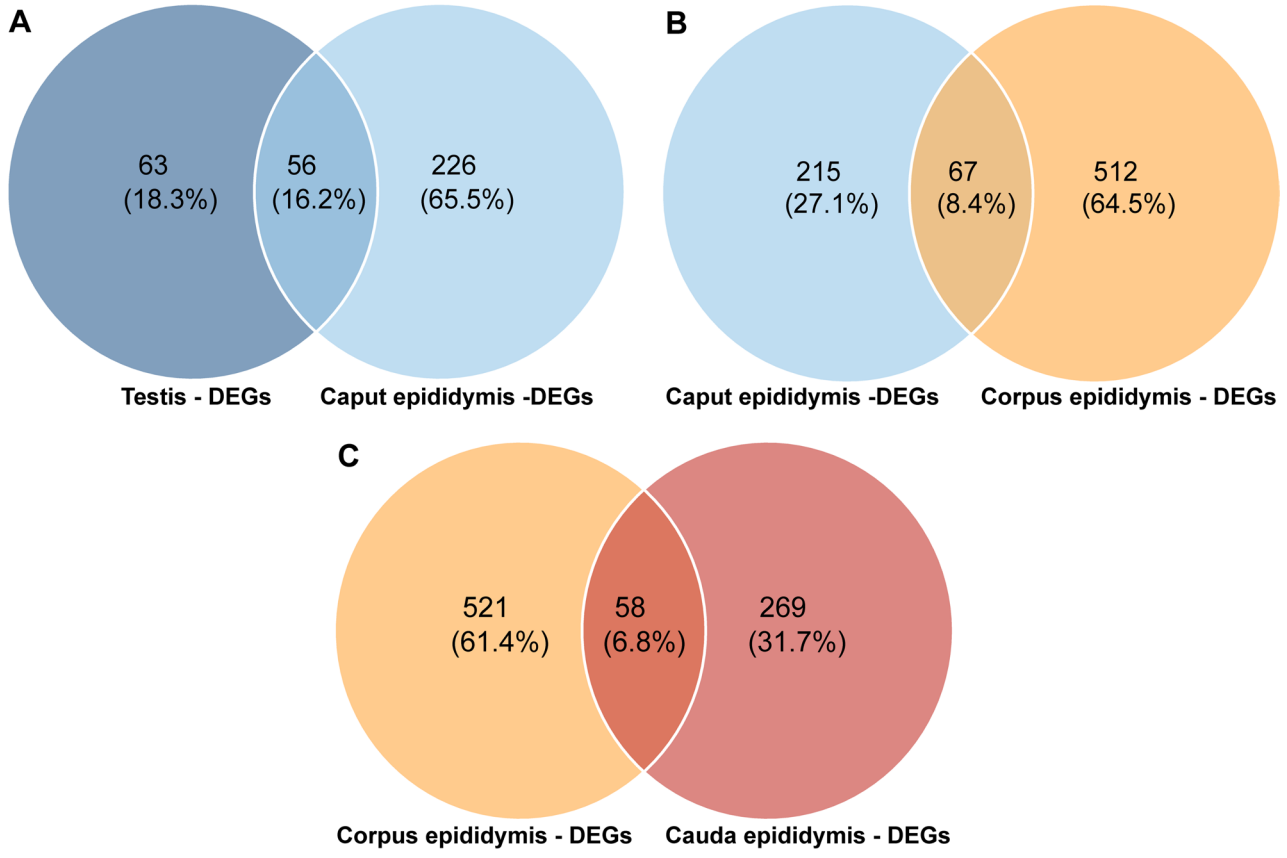

Fig. 4 DEGs between adjacent segments of the testis–epididymis axis. Venn diagrams showing the DEGs between adjacent reproductive regions: **A** testis and caput epididymis, **B** caput and corpus epididymis, **C** corpus and cauda epididymis. Each number represents the count of unique or shared DEGs in the corresponding tissue pair

caput and corpus shared 67 genes (8.4%), and the corpus and cauda epididymis shared 58 genes (6.8%). These findings support the view that each segment of the testis–epididymis axis exhibits distinct transcriptional alterations in response to *CD52* deficiency, consistent with the segment-specific functional enrichment and hub gene profiles identified in earlier analyses.

Discussion

The testis and epididymis play essential and regionally specialized roles in male fertility by coordinating spermatogenesis, sperm maturation, and sperm storage through tissue-specific gene regulation programs. *CD52* has been reported to be expressed in reproductive tissues, however, the region-specific transcriptomic consequences of *CD52* deficiency along the male reproductive tract have not been systematically investigated. In this study, we used CRISPR/Cas9 to generate a *CD52* knockout mouse model and performed a multi-region transcriptomic analysis of the testis and three major epididymal segments. Comparative analyses revealed that *CD52* deficiency was associated with changes in gene expression across all four tissues. Notably, the testis, caput, and cauda epididymis exhibited similar pathway enrichment patterns, whereas the corpus epididymis displayed a distinct transcriptional profile. Moreover, comparisons of differentially expressed genes between adjacent tissues identified both shared and segment-specific changes, indicating spatially heterogeneous transcriptional responses to *CD52* deficiency along the testis–epididymis axis.

CD52 deficiency was associated with transcriptional changes of cytoskeletal, motor protein, and myofibril-related gene sets in the testis, caput, and cauda epididymis. The cytoskeleton, composed of actin filaments, microtubules, and associated proteins, provides the structural framework for intracellular transport and cellular morphogenesis [37]. Motor proteins such as dyneins, kinesins, and myosins generate directional force along these cytoskeletal structures, enabling cargo transport and dynamic cellular remodeling [38–40]. In the testis, actin-based cytoskeletal remodeling is essential for germ cell migration across the seminiferous epithelium, and its disruption can impair spermatogenesis [41–43]. In the epididymis, particularly in the caput and cauda regions, cytoskeletal dynamics support luminal

flow, vesicle-mediated secretion, and the establishment of a microenvironment necessary for sperm maturation. Actin-binding proteins, including motor proteins, are key regulators of these processes and have been implicated in both germ cell development and sperm functional maturation [37, 44–46].

PPI network analysis further identified shared hub genes in the testis, caput, and cauda epididymis following *CD52* deletion. Specifically, *Ttn* emerged as a central node in both the testis and cauda, while *Tcap* was the dominant hub in the caput. Both genes are core components of the sarcomeric cytoskeleton and play roles in stabilizing actin–myosin assemblies and maintaining mechanical tension [47, 48]. Consistent with these structural roles, *Ttn* has been implicated in spermatogenesis and sperm individualization [49], while *Tcap* regulates desmin cytoskeleton organization, with its absence leading to cytoskeletal disruption and mitochondrial dysfunction [50]. The identification of these genes as hub nodes aligns with the enrichment observed in this study. These findings suggest that *CD52* deficiency is associated with transcriptional remodeling of cytoskeleton-related networks in multiple regions of the male reproductive tract.

Unlike the other three tissues, the corpus epididymis exhibited a distinct transcriptomic profile in response to *CD52* deletion, with differentially expressed genes enriched for ion transport, epithelial signaling, and cellular homeostasis-related processes. Consistent with this functional profile, PPI network analysis identified *Spp1* as the central hub gene in this segment. *SPP1* is broadly expressed across the male reproductive system and has been implicated in the regulation of epididymal epithelial and luminal environments [51]. Notably, previous studies have reported pronounced regional specificity of *SPP1* expression within the epididymis across species. In humans, *SPP1* is highly expressed in caput epididymal epithelial cells and is androgen-regulated, supporting a role in epithelial-mediated regulation of the epididymal lumen [52]. Similarly, in mouse models with disrupted epididymal signaling, such as HE6/Gpr64 knockout mice, *Spp1* expression is downregulated in the caput despite preserved tissue morphology [53]. In contrast, studies in dromedary camels have reported higher *Spp1* expression in the corpus epididymis, with corpus-enriched expression positively associated with semen quality in high-fertility individuals. This association has been proposed to involve effects on calcium homeostasis and maintenance of the luminal microenvironment during post-testicular sperm maturation [54]. In addition, *Spp1* and *CD52* have been reported as co-expressed hub genes in calcific aortic valve disease [55], but their regulatory relationship remains unclear. Accordingly, the present data do not establish a direct mechanistic link between *CD52* and *Spp1*. Further targeted functional studies, including cell-type–specific perturbations or combinatorial genetic approaches, will be required to clarify the biological relevance of their potential interaction in the epididymis.

Region-specific gene expression programs along the testis–epididymis axis reflect the distinct functional roles of each tissue in sperm development and maturation [9]. In this study, we demonstrate that *CD52* deficiency is associated with region-specific transcriptional changes across the testis, caput, corpus, and cauda epididymis, highlighting spatial heterogeneity in molecular responses to genetic perturbation. This spatial pattern of transcriptomic divergence is conceptually consistent with recent observations of dynamic small RNA redistribution during post-testicular sperm maturation, in which sperm RNA profiles are transiently remodeled in the caput and partially restored in the cauda [56]. Our study does not directly assess small RNAs or RNA cargo transfer; this parallel highlights shared principles of spatially coordinated and segment-specific regulation along the male reproductive tract. These findings underscore the importance of spatial context in transcriptomic responses to *CD52* deficiency along the male reproductive tract. Future validation studies should therefore take into account the region-dependent expression of *CD52* when interpreting tissue-specific molecular changes.

CD52 deficiency resulted in transcriptomic alterations across the testis and epididymal segments, while CD52-knockout male mice did not exhibit overt abnormalities in reproductive tract morphology and maintained fertility under physiological conditions. These findings are consistent with previous studies using CD52-deficient mice generated by homologous recombination, which also reported no overt reproductive defects [25]. The maintenance of fertility despite transcriptional changes suggests that compensatory or buffering mechanisms may operate within the male reproductive tract. Similar observations have been reported for other non-essential reproductive genes, where genetic disruption results in molecular or transcriptomic alterations without overt impairment of fertility or reproductive tract morphology [57, 58]. We therefore propose that the preserved fertility observed in CD52-deficient mice may reflect a combination of functional redundancy within regulatory networks and tissue-level robustness of the male reproductive tract. Such mechanisms could buffer molecular perturbations and maintain epithelial organization and luminal homeostasis despite the transcriptomic alterations. Future studies employing targeted functional perturbation, pathway-level analysis, or assessment of luminal composition will be required to test these compensatory mechanisms.

This study has several limitations. First, the transcriptomic alterations identified here were not experimentally validated at the RNA or protein level using approaches

such as quantitative PCR, Western blotting, or immunostaining for representative hub genes. Second, bulk RNA sequencing captures average transcriptional changes across heterogeneous cell populations, and it lacks cell-type resolution and temporal information. Given the cellular complexity of the testis and epididymis [59, 60], single-cell or spatial transcriptomic approaches will be required to identify the specific cell populations most responsive to *CD52* deficiency. In addition, functional assays, including sperm motility, capacitation, and fertilization efficiency, will be necessary to determine whether the observed transcriptomic changes have physiological consequences under specific conditions. Despite these limitations, this work established a *CD52* knockout mouse model using CRISPR/Cas9 and provides a comprehensive, region-resolved transcriptomic analysis of *CD52* deficiency across the male reproductive tract.

Conclusion

In summary, using a CRISPR/Cas9-mediated CD52-knockout mouse model, we systematically characterized the transcriptomic responses across the testis and three epididymal segments (caput, corpus, and cauda). *CD52* deficiency altered gene expression in all four tissues, with the testis, caput, and cauda epididymis showing coordinated enrichment in cytoskeletal and motor protein pathways, whereas the corpus displayed a distinct transcriptional profile associated with ion transport and tissue homeostasis. These region-specific responses highlight the spatial heterogeneity of gene regulation along the testis–epididymis axis. Collectively, our findings provide a region-resolved transcriptomic framework for understanding molecular responses to *CD52* deficiency in the male reproductive tract.

Supplementary Information

The online version contains supplementary material available at https://doi.org/10.1186/s12864-026-12652-8.

Supplementary Material 1.

Authors' contributions

HK: Conceptualization, Methodology, Formal analysis, Software, Resources, Data curation, Writing original draft. HK and YZ: Feed animals, Sample collection. FC and HW: Histology analysis, Review, and editing. MG: Supervision, Review, and editing. GH: Methodology, Software, Review, and editing. LH and RC: Methodology, Review and editing, Supervision, Resources.

Funding statement

This research was funded by Shenzhen Municipal Science and Technology Major Projects (KJZD20230923115003006), the Outstanding Talents Training Fund in Shenzhen, Science and Technology Program of Shenzhen (CJGJZD20210408092402006).

Data availability

RNA-seq data generated in this study are available in the NCBI BioProject number PRJNA1257005 (https://www.ncbi.nlm.nih.gov/bioproject/PRJNA1257005).

Declarations

Ethics approval and consent to participate

The C57BL/6J mice used in this study were obtained from Cyagen Biosciences Inc. (Guangzhou, China). The use and care of animals complied with the guidelines of the Biomedical Research Ethics Committee of the Agricultural Genomics Institute in Shenzhen, Chinese Academy of Agricultural Sciences.

Consent for publication

Not applicable.

Competing interests

The authors declare no competing interests.

Author details

[1]Shenzhen Branch, Guangdong Laboratory of Lingnan Modern Agriculture, Key Laboratory of Livestock and Poultry Multi-omics of MARA, Agricultural Genomics Institute at Shenzhen, Chinese Academy of Agricultural Sciences, Shenzhen 518124, China
[2]Animal Breeding and Genomics, Wageningen University & Research, Wageningen, Netherlands
[3]Institute of Sericulture, Chengde Medical University, Chengde, Hebei Province 067000, P. R. China
[4]Agsino Gensources Co., Ltd., Shenzhen 518121, China

Received: 7 October 2025 / Accepted: 11 February 2026
Published online: 16 February 2026

References

1. Nishimura H. L'Hernault SW: spermatogenesis. Curr Biol. 2017;27(18):R988–94.
2. Lv C, Wang X, Guo Y, Yuan S. Role of selective autophagy in spermatogenesis and male fertility. Cells. 2020;9:2523.
3. Griswold MD. Spermatogenesis: the commitment to meiosis. Physiol Rev. 2016;96(1):1–17.
4. Green CD, Ma Q, Manske GL, Shami AN, Zheng X, Marini S, Moritz L, Sultan C, Gurczynski SJ, Moore BB, et al. A comprehensive roadmap of murine spermatogenesis defined by Single-Cell RNA-Seq. Dev Cell. 2018;46(5):651–e667610.
5. Breton S, Nair AV, Battistone MA. Epithelial dynamics in the epididymis: role in the maturation, protection, and storage of spermatozoa. Andrology. 2019;7(5):631–43.
6. Kiyozumi D. Lumicrine signaling: extracellular regulation of sperm maturation in the male reproductive tract lumen. Genes Cells. 2023;28(11):757–63.
7. Zhou W, De Iuliis GN, Dun MD, Nixon B. Characteristics of the epididymal luminal environment responsible for sperm maturation and storage. Front Endocrinol (Lausanne). 2018;9:59.
8. Johnston DS, Jelinsky SA, Bang HJ, DiCandeloro P, Wilson E, Kopf GS, Turner TT. The mouse epididymal transcriptome: transcriptional profiling of segmental gene expression in the epididymis. Biol Reprod. 2005;73(3):404–13.
9. Sipilä P, Björkgren I. Segment-specific regulation of epididymal gene expression. Reproduction. 2016;152(3):R91–99.
10. Gervasi MG, Visconti PE. Molecular changes and signaling events occurring in spermatozoa during epididymal maturation. Andrology. 2017;5(2):204–18.
11. Björkgren I, Sipilä P. The impact of epididymal proteins on sperm function. Reproduction. 2019;158(5):R155–67.
12. Browne JA, Leir SH, Yin S, Harris A. Transcriptional networks in the human epididymis. Andrology. 2019;7(5):741–7.
13. Singh V, Schimenti JC. Relevance, strategies, and added value of mouse models in androgenetics. Andrology. 2025;13(5):1158–69.
14. Jiao SY, Yang YH, Chen SR. Molecular genetics of infertility: loss-of-function mutations in humans and corresponding knockout/mutated mice. Hum Reprod Update. 2021;27(1):154–89.
15. Jiang L, Li T, Zhang X, Zhang B, Yu C, Li Y, Fan S, Jiang X, Khan T, Hao Q. RPL10L is required for male meiotic division by compensating for RPL10 during meiotic sex chromosome inactivation in mice. Curr Biol. 2017;27(10):1498–505. e1496.
16. Miyamoto Y, Sasaki M, Miyata H, Monobe Y, Nagai M, Otani M, Whiley PA, Morohoshi A, Oki S, Matsuda J. Genetic loss of importin α4 causes abnormal sperm morphology and impacts on male fertility in mouse. FASEB J. 2020;34(12):16224–42.

17. Huang Q, Liu Y, Zhang S, Yap YT, Li W, Zhang D, Gardner A, Zhang L, Song S, Hess RA. Autophagy core protein ATG5 is required for elongating spermatid development, sperm individualization and normal fertility in male mice. Autophagy. 2021;17(7):1753–67.
18. Gao Q, Khan R, Yu C, Alsheimer M, Jiang X, Ma H, Shi Q. The testis-specific LINC component SUN3 is essential for sperm head shaping during mouse spermiogenesis. J Biol Chem. 2020;295(19):6289–98.
19. Shah B, Khan R, Shah W, Aftab A, Khan M, Dil S, Shi Q. Inactivation of testis-specific gene C4orf46 is dispensable for spermatogenesis and fertility in mouse. Mamm Genome. 2021;32(5):364–70.
20. Khan M, Jabeen N, Khan T, Hussain H, Ali A, Khan R, et al. The evolutionarily conserved genes: Tex37, Ccdc73, Prss55 and Nxt2 are dispensable for fertility in mice. Sci Rep. 2018;8:4975.
21. Huang Z, Khan M, Xu J, Khan T, Ma H, Khan R, Hussain HMJ, Jiang X, Shi Q. The deubiquitinating gene Usp29 is dispensable for fertility in male mice. Sci China Life Sci. 2019;62:544–52.
22. Xie Y, Khan R, Wahab F, Hussain HMJ, Ali A, Ma H, Jiang H, Xu J, Zaman Q, Khan M. The testis-specifically expressed Dpep3 is not essential for male fertility in mice. Gene. 2019;711:143925.
23. Nie D, Dai Y, Luo Z. The testis-specific expressed gene Spata34 is not required for fertility in mice. Mol Biol Rep. 2020;47(1):285–92.
24. Yousaf A, Wu Y, Khan R, Shah W, Khan I, Shi Q, Jiang X. Normal spermatogenesis and fertility in Ddi1 (DNA damage inducible 1) mutant mice. Reprod Biol. 2020;20(4):520–4.
25. Yamaguchi R, Yamagata K, Hasuwa H, Inano E, Ikawa M, Okabe M. Cd52, known as a major maturation-associated sperm membrane antigen secreted from the epididymis, is not required for fertilization in the mouse. Genes Cells. 2008;13(8):851–61.
26. Pujianto DA, Permatasari S. Mouse CD52 is predominantly expressed in the cauda Epididymis, regulated by androgen and lumicrine factors. J Hum Reprod Sci. 2021;14(4):350–5.
27. Yeung CH, Cooper TG, Nieschlag E. Human epididymal secreted protein CD52 on ejaculated spermatozoa: correlations with semen characteristics and the effect of its antibody. Mol Hum Reprod. 1997;3(12):1045–51.
28. Luo J, Zhu S, Kang Y, Liu X, Tan X, Zhao J, Ding X, Li H. Isolation of CD63-positive epididymosomes from human semen and its application in improving sperm function. J Extracell Vesicles. 2024;13(10):e70006.
29. Yang H, Wang H, Jaenisch R. Generating genetically modified mice using CRISPR/Cas-mediated genome engineering. Nat Protoc. 2014;9(8):1956–68.
30. Chen S, Zhou Y, Chen Y, Gu J. Fastp: an ultra-fast all-in-one FASTQ preprocessor. Bioinformatics. 2018;34(17):i884–90.
31. Dobin A, Davis CA, Schlesinger F, Drenkow J, Zaleski C, Jha S, Batut P, Chaisson M, Gingeras TR. STAR: ultrafast universal RNA-seq aligner. Bioinformatics. 2013;29(1):15–21.
32. Li B, Dewey CN. RSEM: accurate transcript quantification from RNA-Seq data with or without a reference genome. BMC Bioinformatics. 2011;12:323.
33. Love MI, Huber W, Anders S. Moderated Estimation of fold change and dispersion for RNA-seq data with DESeq2. Genome Biol. 2014;15(12):550.
34. Wu T, Hu E, Xu S, Chen M, Guo P, Dai Z, Feng T, Zhou L, Tang W, Zhan L, et al. ClusterProfiler 4.0: A universal enrichment tool for interpreting omics data. Innov (Camb). 2021;2(3):100141.
35. Szklarczyk D, Kirsch R, Koutrouli M, Nastou K, Mehryary F, Hachilif R, Gable AL, Fang T, Doncheva NT, Pyysalo S, et al. The STRING database in 2023: protein-protein association networks and functional enrichment analyses for any sequenced genome of interest. Nucleic Acids Res. 2023;51(D1):D638–46.
36. Chin CH, Chen SH, Wu HH, Ho CW, Ko MT, Lin CY. CytoHubba: identifying hub objects and sub-networks from complex interactome. BMC Syst Biol. 2014;8(Suppl 4):S11.
37. Dunleavy JEM, O'Bryan MK, Stanton PG, O'Donnell L. The cytoskeleton in spermatogenesis. Reproduction. 2019;157(2):R53–72.
38. Howard J. Molecular mechanics of cells and tissues. Cell Mol Bioeng. 2008;1:24–32.
39. Wen Q, Tang EI, Xiao X, Gao Y, Chu DS, Mruk DD, Silvestrini B, Cheng CY. Transport of germ cells across the seminiferous epithelium during spermatogenesis—the involvement of both actin-and microtubule-based cytoskeletons. Tissue Barriers. 2016;4(4):e1265042.
40. Khosravanizadeh A, Dmitrieff S. Dynamic clamping induces rotation-to-beating transition of pinned filaments in gliding assays. J R Soc Interface. 2025;22(226):20240859.
41. Kierszenbaum AL, Tres LL. The acrosome-acroplaxome-manchette complex and the shaping of the spermatid head. Arch Histol Cytol. 2004;67(4):271–84.
42. Flaherty SP, Winfrey VP, Olson GE. Localization of actin in mammalian spermatozoa: a comparison of eight species. Anat Rec. 1986;216(4):504–15.
43. Tachibana M, Terada Y, Murakawa H, Murakami T, Yaegashi N, Okamura K. Dynamic changes in the cytoskeleton during human spermiogenesis. Fertil Steril. 2005;84:1241–8.
44. Sun X, Kovacs T, Hu YJ, Yang WX. The role of actin and myosin during spermatogenesis. Mol Biol Rep. 2011;38(6):3993–4001.
45. Wang L, Yan M, Wu S, Wu X, Bu T, Wong CKC, Ge R, Sun F, Cheng CY. Actin binding proteins, actin cytoskeleton and spermatogenesis - Lesson from toxicant models. Reprod Toxicol. 2020;96:76–89.
46. Yang T, Yang WX. The dynamics and regulation of microfilament during spermatogenesis. Gene. 2020;744:144635.
47. Gregorio CC, Trombitás K, Centner T, Kolmerer B, Stier G, Kunke K, Suzuki K, Obermayr F, Herrmann B, Granzier H, et al. The NH2 terminus of Titin spans the Z-disc: its interaction with a novel 19-kD ligand (T-cap) is required for sarcomeric integrity. J Cell Biol. 1998;143(4):1013–27.
48. Valle G, Faulkner G, De Antoni A, Pacchioni B, Pallavicini A, Pandolfo D, Tiso N, Toppo S, Trevisan S, Lanfranchi G. Telethonin, a novel sarcomeric protein of heart and skeletal muscle. FEBS Lett. 1997;415(2):163–8.
49. Chauveau C, Rowell J, Ferreiro A. A rising titan: TTN review and mutation update. Hum Mutat. 2014;35(9):1046–59.
50. Furukawa T, Ono Y, Tsuchiya H, Katayama Y, Bang ML, Labeit D, Labeit S, Inagaki N, Gregorio CC. Specific interaction of the potassium channel beta-subunit MinK with the sarcomeric protein T-cap suggests a T-tubule-myofibril linking system. J Mol Biol. 2001;313(4):775–84.
51. Rashad DEM, Ibrahim S, El-Sokary MMM, Mahmoud KGM, Abou El-Roos MEA, Sosa GAM, Kandiel MMM. Abundance of selected genes implicated in testicular functions in Camelus dromedarius with high and low epididymal semen quality. Biol Reprod. 2024;110(3):501–8.
52. Browne JA, Yang R, Leir SH, Eggener SE, Harris A. Expression profiles of human epididymis epithelial cells reveal the functional diversity of caput, corpus and cauda regions. Mol Hum Reprod. 2016;22(2):69–82.
53. Davies B, Behnen M, Cappallo-Obermann H, Spiess AN, Theuring F, Kirchhoff C. Novel epididymis-specific mRNAs downregulated by HE6/Gpr64 receptor gene disruption. Mol Reprod Dev. 2007;74(5):539–53.
54. Rashad DEM, Ibrahim S, El-Sokary MMM, Mahmoud KGM, Kandiel MMM, Abou El-Roos MEA, Sosa GAM. Region-specific gene expression profile in the epididymis of high- and low-fertile dromedary camels. Reprod Domest Anim. 2024;59(7):e14678.
55. Sun JY, Hua Y, Shen H, Qu Q, Kan JY, Kong XQ, Sun W, Shen YY. Identification of key genes in calcific aortic valve disease via weighted gene co-expression network analysis. BMC Med Genomics. 2021;14(1):135.
56. Wang H, Wang Z, Zhou T, Morris D, Chen S, Li M, Wang Y, Zheng H, Fu W, Yan W. Small RNA shuffling between murine sperm and their cytoplasmic droplets during epididymal maturation. Dev Cell. 2023;58(9):779–e790774.
57. Xia B, Yan Y, Baron M, Wagner F, Barkley D, Chiodin M, Kim SY, Keefe DL, Alukal JP, Boeke JD. Widespread transcriptional scanning in the testis modulates gene evolution rates. Cell. 2020;180(2):248–62. e221.
58. Láruson ÁJ, Yeaman S, Lotterhos KE. The importance of genetic redundancy in evolution. Trends Ecol Evol. 2020;35(9):809–22.
59. Zhang G, Sun Y, Guan M, Liu M, Sun S. Single-cell and Spatial transcriptomic investigation reveals the Spatiotemporal specificity of the beta-defensin gene family during mouse sperm maturation. Cell Commun Signal. 2024;22(1):267.
60. Liu MM, Fan CQ, Zhang GL. A single-cell landscape of spermioteleosis in mice and pigs. Cells. 2024;13:563.

Publisher's note